BIOCHEMISTRY
including biophysical chemistry & molecular biology

ARTICLE

pubs.acs.org/biochemistry

# Activation of Cell Death Mediated by Apoptosis-Inducing Factor Due to the Absence of Poly(ADP-ribose) Glycohydrolase

Yiran Zhou, Xiaoxing Feng, and David W. Koh*

Department of Pharmaceutical Sciences, College of Pharmacy, Washington State University, Pullman, Washington 99164, United States

Supporting Information

**ABSTRACT:** We previously demonstrated that the absence of poly(ADP-ribose) glycohydrolase (PARG) led to increased cell death following DNA-damaging treatments. Here, we investigated cell death pathways following UV treatment. Decreased amounts of PARG-null embryonic trophoblast stem (TS) cells were observed following doses of 10−100 J/m$^2$ as compared to wild-type cells. In wild-type cells, caspase-cleaved poly(ADP-ribose) polymerase-1 (PARP-1) and activated caspase-3 were detected 12−24 h after UV treatment. Surprisingly, both were detected at decreased levels only after 24 h in PARG-null TS cells, indicating a decreased level and delayed presence of caspase-mediated events. Further, a time- and dose-dependent accumulation of poly(ADP-ribose) (PAR) levels after UV was observed in PARG-null TS cells and not in wild-type cells. Determination of the levels of nicotinamide adenine dinucleotide ($NAD^+$), the substrate for PAR synthesis and a coenzyme in cellular redox reactions, demonstrated a UV dose-dependent decrease in the level of $NAD^+$ in wild-type cells, while $NAD^+$ levels in PARG-null TS cells remained at higher levels. This indicates no depletion of $NAD^+$ in PARG-null TS cells following increased levels of PAR. Lastly, cell death mediated by apoptosis-inducing factor (AIF) was analyzed because of its dependence on increased PAR levels. The results demonstrate nuclear AIF translocation only in PARG-null TS cells, which demonstrates the presence of AIF-mediated cell death. Herein, we provide compelling evidence that the absence of PARG leads to decreased caspase-3 activity and the specific activation of AIF-mediated cell death. Therefore, the absence of PARG may provide a strategy for specifically inducing an alternative apoptotic pathway.

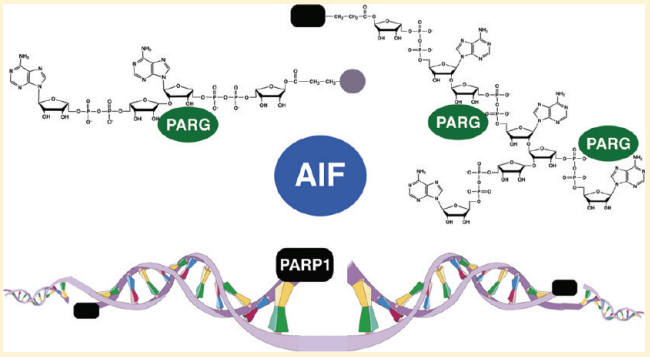


The maintenance of genomic integrity by poly(ADP-ribose) (PAR) following DNA damage is based in part on its ability to facilitate DNA repair or promote cell death. The majority of PAR is synthesized by PAR polymerase-1 (PARP-1).[1] In response to DNA damage, PARP-1 utilizes the coenzyme nicotinamide adenine dinucleotide ($NAD^+$) as a substrate to catalyze the covalent modification of nuclear acceptor proteins with PAR.[2] PAR is removed from acceptor proteins by the activity of PAR glycohydrolase (PARG), which catalyzes the hydrolysis of PAR into free ADP-ribose with high specific activity.[3] PAR synthesis and degradation are closely coordinated events, which result in a transient existence of PAR.[4] Recent studies demonstrate that elevated levels of PAR, due to the inhibition or genetic knockdown of PARG, lead to cell death.[5−7] We previously demonstrated that elevated levels of PAR due to the complete absence of PARG cause embryonic lethality in vivo[8] and increased levels of DNA damage and cell death in vitro.[8,9]

PAR appears to have a role in several pathways of cell death. The involvement of PAR in cell death was initially associated with necrosis, as high levels of PAR were thought to deplete cellular levels of $NAD^+$,[10] the substrate for PAR synthesis and a coenzyme required for mitochondrial redox reactions. The importance of this type of cell death was demonstrated in the pathogenesis of ischemic injury[11,12] and in cell death due to chemotherapy.[13] PAR was also associated with caspase-dependent apoptosis due to the specific cleavage of PARP-1 into 24 and 89 kDa forms by caspase-3 during apoptosis.[14] However, cells lacking PARP-1 were shown to undergo caspase-dependent apoptosis normally following stimuli that activate intrinsic or extrinsic apoptotic pathways.[15] Subsequent studies were suggestive of a role for PAR in apoptotic pathways.[16,17] To date, a direct role for PAR metabolism in caspase-dependent apoptosis has not been identified.

However, PAR was subsequently demonstrated to be essential for the ability of apoptosis-inducing factor (AIF), a pro-apoptotic mitochondrial protein, to initiate cell death.[18] Following cell death stimuli, AIF translocates to the nucleus to initiate apoptosis.[19] A recent study reveals that in the nucleus, AIF associates with histone H2AX and cyclophilin A (CypA) to form a DNA-fragmenting complex that is essential for initiating programmed cell death through this pathway.[20] Initial studies demonstrated that the ability of AIF to induce cell death was caspase-independent,[19,21] while subsequent studies demonstrated it was

**Received:** November 16, 2010
**Revised:** February 16, 2011
**Published:** March 02, 2011

caspase-dependent.[22,23] To date, cell death studies support the possibility that AIF may contribute to caspase-dependent apoptosis and induce an alternative form of cell death that is caspase-independent.[24] Moreover, AIF functionality does appear to be dependent on PAR, because AIF fails to translocate in the absence of PAR synthesis.[18,25] Further, the delivery of purified PAR to cultured cells induces AIF translocation.[26] Therefore, it appears that cell death by PAR involves elevated levels of nuclear PAR, nuclear-to-mitochondrial PAR signaling, and cell death mediated by AIF. Thus, increasing PAR levels may provide a novel method for promoting AIF-mediated cell death.

Although an ADP-ribose hydrolase-like (ARH3) protein has also been shown to catalyze the hydrolysis of PAR in vitro,[27] PARG is the primary enzyme known to catalyze hydrolysis of PAR in vivo. The absence of PARG leads to elevated levels of intranuclear PAR and an increased level of cell death.[8,28] A recent study reveals that the specific knockdown of nuclear PARG leads to a decreased level of DNA repair and increased genomic instability.[29] Because PARG appears to be the primary regulator of PAR levels in the cell and its absence leads to deleterious consequences, it may also regulate the initiation of cell death via AIF. Thus, the inhibition of PAR hydrolysis via inhibition of PARG is potentially a means of triggering the AIF cell death pathway.

We show here that the absence of PARG led to decreased levels of activated caspase-3 and caspase-cleaved PARP-1 following UV treatment. Also, UV treatment led to increased levels of PAR in PARG-null trophoblast stem (TS) cells. Although PAR levels were increased, cellular $NAD^+$ levels were also increased in PARG-null TS cells as compared to wild-type cells. These increases in PAR levels and $NAD^+$ were coincident with the detection of AIF in the nuclei of PARG-null TS cells. Because these effects were observed in only PARG-null TS cells, our results demonstrate that the absence of PARG leads to the activation of AIF-mediated cell death following UV radiation.

## EXPERIMENTAL PROCEDURES

**Materials.** RPMI 1640 medium and fetal bovine serum (FBS) were purchased from Hyclone (Logan, UT). Heparin sodium, benzamide, Hoechst 33342 (bis-benzimide H 33342 trihydrochloride), 4′,6-diamidino-2-phenylindole (DAPI), $NAD^+$, and alcohol dehydrogenase (ADH) were purchased from Sigma (St. Louis, MO). Annexin-V fluorescein (FITC) conjugate was purchased from Southern Biotech (Birmingham, AL). Protease inhibitor cocktail tablets (Complete Mini, EDTA-free) were from Roche (Mannheim, Germany). Recombinant human fibroblast growth factor-4 and the caspase inhibitor, Q-VD-OPh, were purchased from R&D Systems (Minneapolis, MN). The following primary antibodies were used: monoclonal anti-cyclobutane pyrimidine dimer (CPD) (Cosmo Bio USA, West Carlsbad, CA), polyclonal anti-cleaved PARP-1 (Asp214) (Cell Signaling, Danvers, MA), monoclonal anti-caspase-3 clone 8G10 (Cell Signaling), polyclonal anti-PAR (Trevigen, Gaithersburg, MD), polyclonal anti-$\beta$-tubulin (Sigma), polyclonal anti-$\beta$-actin (Millipore, Billerica, MA), polyclonal anti-AIF (Rockland Immunochemicals, Gilbertsville, PA), polyclonal anti-manganese superoxide dismutase (MnSOD) (Millipore), and monoclonal anti-lamin B2 clone LN43 (Thermo Fisher, Pittsburgh, PA). Horseradish peroxidase (HRP)-conjugated goat anti-rabbit and anti-mouse (Sigma) and Oregon Green-conjugated anti-mouse (Invitrogen, Carlsbad, CA) secondary antibodies were used.

**Embryonic Trophoblast Stem (TS) Cell Culture.** Wild-type and PARG-null embryonic TS cells were derived from E3.5 mouse blastocysts as previously described.[8] PARG-null TS cells are completely devoid of PARG mRNA and protein, and they must be maintained in growth medium containing fibroblast growth factor-4, heparin sodium, murine embryonic feeder (MEF)-conditioned medium, 15% FBS, and 0.5 mM benzamide (BZ, a PAR synthesis inhibitor) for long-term viability. Both wild-type and PARG-null TS cells were grown and maintained in medium containing BZ. In the 2 day period during which BZ is withdrawn for most studies, levels of PAR in PARG-null TS cells slowly increase, but cell death is at a minimum (10−15%).[8] As a precaution, because of long-term exposure to BZ, cell lines are periodically rederived.

**Detection of CPDs following UV Radiation.** UV-C was utilized because of its ability to efficiently cause DNA lesions repaired by the nucleotide excision repair (NER) pathway.[30,31] In addition, the cells utilized are cultured in BZ, which inhibits the PARPs, as well as DNA base excision repair (BER).[32] Thus, we also chose to utilize UV-C to avoid any effects due to the inhibition of BER. TS cells were treated with UV radiation as described previously.[9] Briefly, cells were cultured with or without BZ for 2 days on glass coverslips and treated with UV radiation using a low-pressure Hg lamp (model G30T8, Sylvania, Danvers, MA) at 10−100 J/m$^2$ (these doses of UV-C are not physiologically relevant, but in addition to the reasons stated above, UV-C was chosen to study the mechanisms of PARP/PARG in response to UV-induced DNA damage). The cells were fixed with 4% formalin for 10 min, washed with PBS, permeabilized with 0.5% Triton X-100 for 5 min, and washed again. After treatment with 2 M HCl for 30 min, cells were washed, blocked with a 10% BSA/PBS mixture for 30 min, and incubated for 2 h at 37 °C with monoclonal anti-CPD antibody (1:1500) in a 3% BSA/PBS mixture. After three washes, cells were incubated with Oregon Green-conjugated anti-mouse antibody (1:1000) in a 3% BSA/PBS mixture for 45 min at 37 °C, washed again with PBS, and mounted on glass microscope slides containing DAPI. Immunocytochemistry analysis was then performed by confocal microscopy.

**Cell Counts.** TS cells were seeded at a density of $1 \times 10^5$ cells/well in 24-well plates. After 20−24 h, cells were stained with DAPI and images were obtained using a Zeiss Axio Observer Z1 inverted fluorescent microscope with a Hamamatsu Orca-ER CCD camera. At least six images were obtained per well. Mean cell counts for each UV dose for wild-type and PARG-null TS cells without BZ were obtained. Cell counts for untreated wells were designated as 100% cell survival. Cell counts for UV-treated wells were calculated as a percentage of untreated cell counts. Error bars were calculated as the standard error of the mean (SEM). One-way analysis of variance (ANOVA) and an unpaired Student's $t$ test were then performed (wild type without BZ vs PARG-null without BZ).

**Quantification of Cell Death.** TS cells were grown with or without BZ for 2 days in 24-well plates and treated with 10−100 J/m$^2$ UV radiation. The cells were immediately washed once with PBS and incubated in growth medium at 37 °C. Twenty hours later, cells were harvested with trypsin, washed with PBS, and resuspended in PBS. Cell suspensions were then stained with annexin V-FITC according to the manufacturer's protocol and analyzed by FACS as described previously.[9]

**Immunoblotting Analyses.** Wild-type and PARG-null TS cells were treated with UV radiation as described above in 60 mm

tissue culture dishes. For caspase inhibition, cells were pretreated with 40 $\mu$M Q-VD-OPh, a broad-spectrum, irreversible caspase inhibitor,[33] for 30 min before UV exposure and maintained in growth medium containing the same dose of Q-VD-OPh for 24 h after treatment. Cells were harvested by scraping, washed with PBS, resuspended in lysis buffer containing 10 mM Tris-HCl (pH 8), 150 mM NaCl, 1 mM EDTA, 1 mM EGTA, and protease inhibitors (Complete Mini, EDTA-free), and lysed by brief sonication (5 s, 10% intensity). The crude lysates were clarified by centrifugation (16000*g* for 15 min at 4 °C), 20 $\mu$g of each cleared lysate was subjected to 12% sodium dodecyl sulfate−polyacrylamide gel electrophoresis (SDS−PAGE), and the proteins were transferred to nitrocellulose by semidry transfer (25 V for 30 min) using a Trans-blot SD apparatus (Bio-Rad, Hercules, CA). For anti-PAR immunoblot after 10−100 J/m$^2$ UV treatments, 7.5% SDS−PAGE was used. Membranes were blocked with PBS and 0.1% Tween 20 (PBS-Tween) containing 5% milk for 1 h and incubated with the primary antibody (1:1000) overnight at 4 °C. Membranes were then washed with PBS-Tween three times and incubated with HRP-conjugated goat anti-rabbit or anti-mouse antibody (1:10000) for 1 h. The blot was washed as described above, and chemiluminescence was initiated using the Supersignal West Pico reagents (Pierce, Rockford, IL). Immunoblots were then developed by film or on a Chemidoc gel imager (Bio-Rad).

For quantification of protein bands, immunoblots were examined by densitometry with the Chemidoc imager using Quantity One according to the manufacturer's recommended settings. Each trace was corrected for background via subtraction of an equivalent tracing of a non-antigenic region for that blot. Protein bands from at least two immunoblots were quantified for each data point. Error bars were calculated as SEM.

**Caspase Activity Assay.** Wild-type and PARG-null TS cells were cultured without BZ for 2 days and treated with 25 J/m$^2$ UV radiation. Twelve hours after being treated, approximately 1 × 10$^5$ cells were subjected to the Apo-ONE Homogeneous Caspase-3/7 Assay (Promega) according to the manufacturer's specifications. This assay consists of the rhodamine-labeled profluorescent caspase-3/7 substrate, bis(*N*-carbobenzyloxy-L-aspartyl-L-glutamyl-L-valylaspartic acid amide) (Z-DEVD), that becomes fluorescent upon cleavage by caspase-3/7 enzymes. The amount of fluorescent product generated is representative of the amount of active caspase-3/7 present in the cells. Plates were analyzed with a Bio-Tek (Winooski, VT) Synergy HT plate reader at an excitation wavelength of 485 nm and at an emission wavelength of 527 nm. Total caspase-3/7 activity was expressed as a percentage of caspase-3/7 activity in untreated cells. Negative controls were provided by untreated cells and cells pretreated with Q-VD-OPh as previously described. Samples were analyzed in duplicate, and at least two independent experiments were performed.

**Subcellular Fractionations.** For the fractionation of wild-type and PARG-null TS cells, the cells were grown to confluence in 100 mm tissue cultures dishes and washed twice with ice-cold PBS. The cells were harvested by being scraped in ice-cold PBS and centrifuged at 720*g* for 3 min. The pellet was resuspended in hypotonic homogenization buffer containing 10 mM Tris-HCl (pH 7.4), 10 mM KCl, 1.5 mM $MgCl_2$, 1 mM EDTA sodium, 1 mM EGTA, 0.1 mM PMSF, and a protease inhibitor mixture (Complete Mini, EDTA-Free, Roche) and left on ice for 30 min. NP-40 was added to a final concentration of 0.1%, and the cells were homogenized with 40 strokes in a 2 mL Dounce homogenizer using the B-type pestle. The nuclear fraction was obtained by centrifugation at 720*g* for 5 min. The supernatant was collected and designated as the postnuclear fraction (cytoplasm and mitochondria). The nuclear fraction was washed twice with isotonic buffer (hypotonic buffer and 0.25 M sucrose) and resuspended in PBS with 0.1% NP-40.

**Assay for NAD$^+$ Content.** Approximately 20−24 h after UV treatment, the total cellular NAD$^+$ content was quantified using the ADH cycling assay.[34] Briefly, wild-type and PARG-null TS cells in 24-well plates were washed with ice-cold PBS and harvested with 0.5 mL of 1 M NaOH. Immediately afterward, 0.125 mL of 2 M $H_3PO_4$ was added and an equal volume of 1 M $HClO_4$ was added for protein precipitation. The samples were left on ice for 10 min and centrifuged (800*g* for 4 °C at 10 min). The pellet was used to quantify total protein (BCA assay kit, Pierce). The supernatant (1 mL) was removed; 0.5 mL of 1 M KOH was added, and the sample was centrifuged as described above. The resulting supernatant was used for NAD$^+$ quantification using a 96-well microplate NAD$^+$ assay.[34] The total NAD$^+$ content was expressed as picomoles of NAD$^+$ per microgram of protein. This normalization of NAD$^+$ levels was required to account for any differences in cell number, which would be reflected in higher or lower protein levels. All samples were quantified in triplicate, and three independent experiments were performed. Error bars represent the SEM. One-way ANOVA and an unpaired Student's *t* test were then performed (wild type with BZ vs wild type without BZ; PARG-null with BZ vs PARG-null without BZ).

## RESULTS

**Decreased Amounts of PARG-Null TS Cells without BZ following UV Irradiation.** We previously generated PARG-null TS cells via the genetic disruption of the *Parg* gene.[8] These cells were characterized and found to be completely devoid of PARG mRNA and protein. The total PAR hydrolytic activity is significantly decreased, but not absent, in PARG-null TS cells, which most likely reflects a low level of PAR hydrolysis due to ARH3 (data not shown). However, it does not appear that this low level of PAR hydrolysis is sufficient to regulate PAR, as elevated levels of PAR were observed in PARG-null TS cells without BZ in previous studies.[8,9] Because the accumulation of PAR leads to cytotoxicity, PARG-null TS cells must be maintained in growth medium containing the PAR synthesis inhibitor, benzamide (BZ, 0.5 mM), for long-term viability. We also previously reported the enhanced accessibility of DNA-damaging agents and UV radiation to DNA in the absence of PARG.[9] To further examine UV-induced DNA damage and cell death, we compared the amount of DNA damage and cell survival after treating wild-type cells with 25 J/m$^2$ and PARG-null TS cells with 10 J/m$^2$ of UV radiation. Wild-type and PARG-null TS cells were grown in medium without BZ for 2 days and treated with the different doses of UV radiation. These treatments led to increased levels of DNA damage in both groups as demonstrated by the increased amount of CPDs detected by immunocytochemistry (Figure 1A). In wild-type TS cells 24 h later, a decreased amount of CPDs was detected, indicating successful DNA nucleotide excision repair (NER). However, in PARG-null TS cells after 24 h, a decreased amount of CPDs was detected as well, but fewer cells remained as compared to the number in wild-type cells (Figure 1A). This suggests a decreased level of cell survival in PARG-null TS cells following 10 J/m$^2$ of UV radiation, as compared to a higher level of cell survival in wild-type

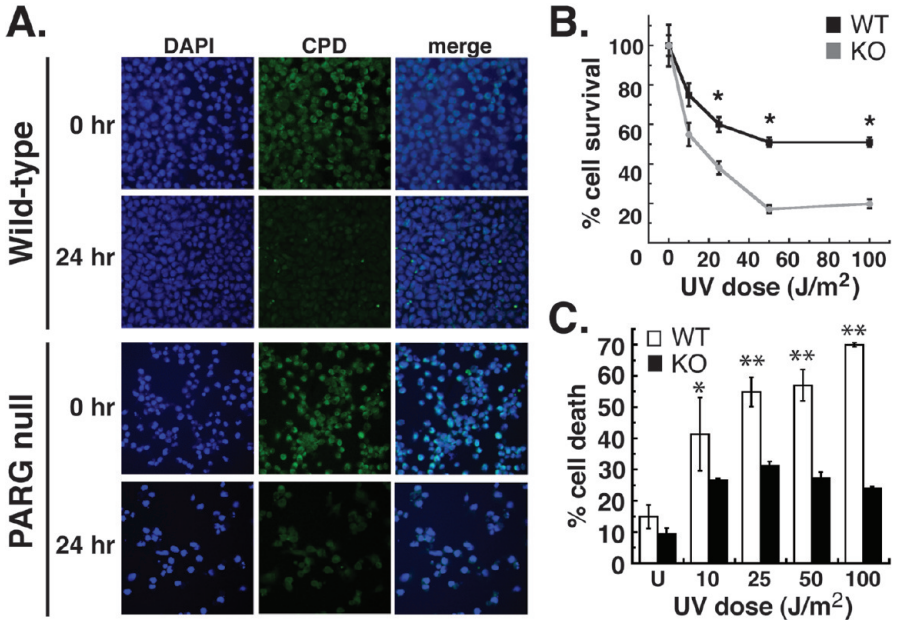


**Figure 1.** Treatment of wild-type and PARG-null TS cells with UV radiation. Wild-type (WT) and PARG-null (KO) TS cells were cultured without BZ for 2 days. (A) Wild-type TS cells were treated with 25 J/m$^2$ of UV-C radiation, and PARG-null TS cells were treated with a dose of 10 J/m$^2$. After being treated for 0 and 24 h, cells were analyzed by immunocytochemistry for DNA damage using a monoclonal antibody specific for cyclobutane pyrimidine dimers (CPDs) (Cosmo Bio USA). Cells were then incubated with Oregon Green-conjugated anti-mouse antibody (1:1000). The detection of nuclei was achieved via DAPI staining. (B) Twenty-four hours after treatments, cell survival was assessed by counting DAPI-stained nuclei following UV treatment and expressing these values as a percent of untreated cell counts. *$P$ < 0.01 between WT-BZ and KO-BZ (one-way ANOVA and unpaired Student's $t$ test). (C) Twenty hours after UV treatment, apoptotic cell death was assessed by annexin-V-FITC staining of TS cells and subsequent analysis by FACS. *$P$ < 0.05 and **$P$ < 0.01 between WT-BZ and KO-BZ (one-way ANOVA and unpaired Student's $t$ test). For panels B and C, each sample was counted in triplicate and error bars represent SEM. All experiments were repeated at least twice with similar results.

cells following 25 J/m$^2$ of UV radiation. Further analysis involved the treatment of wild-type and PARG-null TS cells with 10−100 J/m$^2$ of UV radiation and quantifying cell survival (Figure 1B). Cell survival was quantified by obtaining cell counts following DAPI staining of nuclei and expressing these counts as a percentage of the total number of untreated cells. The results demonstrate a decreased amount of PARG-null TS cells at each UV dose as compared to the amount of wild-type cells, which indicates the decreased level of survival of PARG-null TS cells. Quantification of cell death by annexin-V staining demonstrated a decreased level of annexin-V labeling of PARG-null TS cells as compared to wild-type cells (Figure 1C). Because annexin-V binds phosphatidylserine on the cell surface,[35] which is a common morphological feature in caspase-dependent apoptosis,[36] this result suggests less cell death in PARG-null TS cells due to caspases. Because PARG-null TS cells exhibit less survival at each UV dose (Figure 1B), the results also suggest that PARG-null TS cells undergo an alternative pathway of cell death due to UV. These results therefore suggest that the absence of PARG leads to an increased level of cell death due to an alternative pathway following UV radiation.

**Decreased Levels of Cleaved PARP-1 and Activated Caspase-3 in PARG-Null TS Cells without BZ following UV Irradiation.** To investigate cell death pathways in the absence of PARG, wild-type and PARG-null TS cells were treated with 25 J/m$^2$ of UV radiation and cell lysates were analyzed by Western blotting for cleaved PARP-1 and caspase-3 at 0−24 h time points (Figure 2). During caspase-mediated apoptosis, PARP-1 is cleaved to a 89 kDa form by caspase-3.[14] Following UV treatment, the presence of cleaved PARP-1 peaked at 12 and 24 h in wild-type TS cells with or without BZ as displayed by immunoblotting (Figure 2A,a) and densitometry (Figure 2C, a). In PARG-null TS cells with BZ, levels of cleaved PARP-1 were also maximal at 12 and 24 h, although low levels of cleaved PARP-1 were also detected 0 and 6 h after UV treatment (Figure 2B,a and Figure 2C,a). These observations of cleaved PARP-1 at 12 and 24 h were consistent with the presence of activated caspase-3. Caspase-3 is present in the cell in a nonactive 32 kDa procaspase form, but following apoptotic stimuli, it is processed to 17 and 12 kDa fragments that ultimately lead to an active complex that catalyzes the proteolysis of downstream protein targets.[37] In wild-type TS cells with or without BZ, the 32 kDa procaspase form was present at all time points (Figure 2A,b), but the 17 kDa activated caspase-3 fragment was observed at only 12 and 24 h (Figure 2A,c and Figure 2C,b), which correlates with the maximal levels of cleaved PARP-1 in these cells (Figure 2A,a and Figure 2C,a). This fragment was also detected in PARG-null TS cells with BZ at 6−24 h (Figure 2B,c and Figure 2C,b), which correlated with the presence of cleaved PARP-1 in these cells (Figure 2B,a and Figure 2C,a). No activated caspase-3 was observed in untreated wild-type or PARG-null TS cells (Figure 2A,c and Figure 2B,c, lane U) or UV-treated cells pretreated with the broad-spectrum caspase inhibitor, Q-VD-OPh (Figure 2, Q). However, in PARG-null TS cells without BZ, cleaved PARP-1 was not observed until 24 h after UV treatment (Figure 2B,a). Analysis by densitometry confirmed the presence of cleaved PARP-1 only at 24 h (Figure 2C,b). These results correlated with the presence of activated caspase-3 at 24 h (Figure 2B,c and Figure 2C,b). Further, both were present at decreased levels compared to the levels in wild-type TS cells with or without BZ and PARG-null TS cells with BZ at 12 and 24 h.

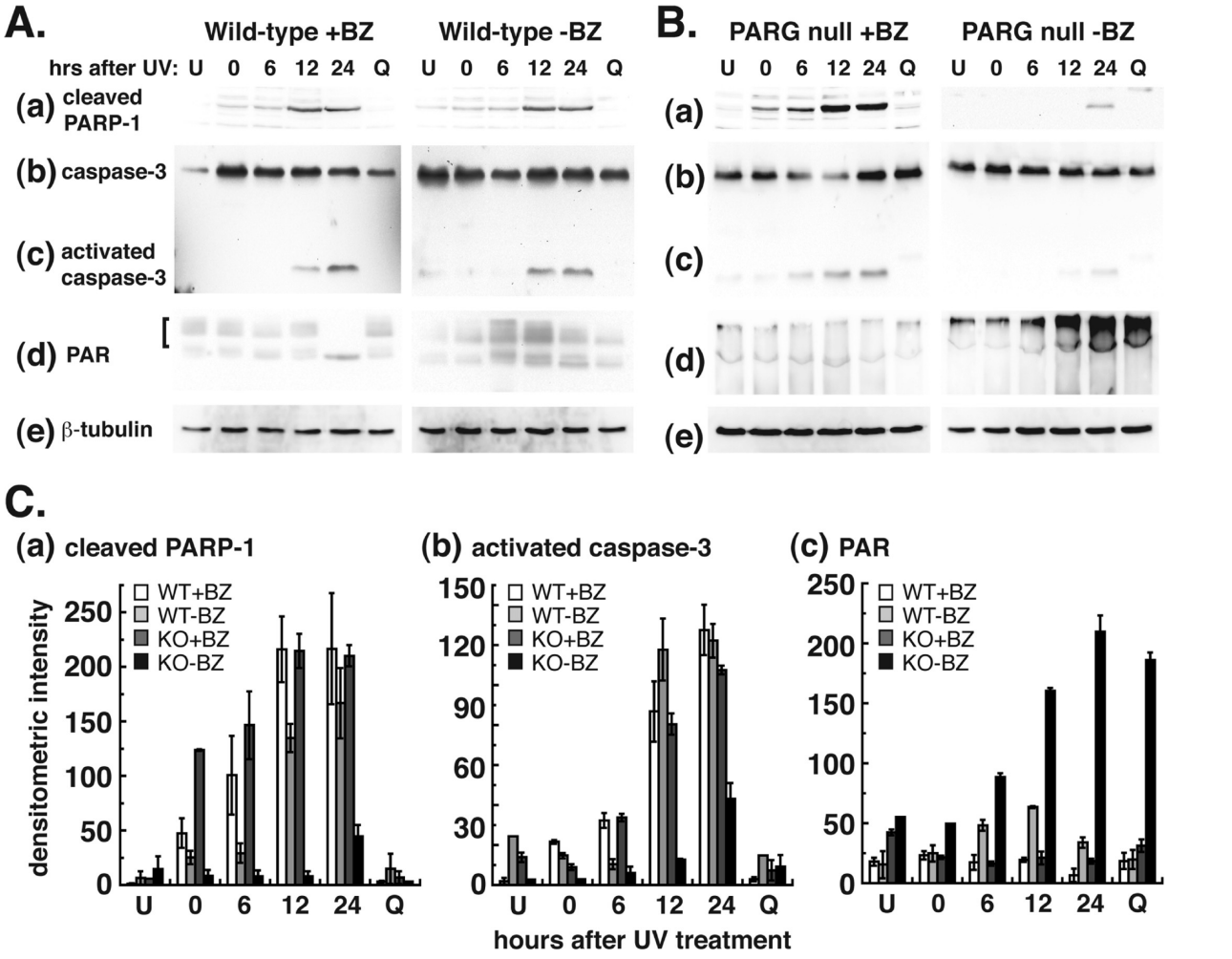


**Figure 2.** Immunoblotting analysis of cleaved PARP-1, caspase-3, and PAR in PARG TS cells after UV radiation. Wild-type (A) and PARG-null TS (B) cells were grown with or without BZ for 2 days and treated with 25 J/m$^2$ of UV radiation. From 0 to 24 h after treatment, cell lysates were analyzed by immunoblot detection for (a) cleaved PARP-1 (monoclonal anti-89 kDa PARP-1, Cell Signaling), (b) procaspase-3 (32 kDa), (c) activated caspase-3 (17 kDa) (monoclonal anti-caspase 3, clone 8G10, Cell Signaling), (d) PAR (polyclonal anti-PAR, clone 96-10, Trevigen), and (e) $\beta$-tubulin (monoclonal anti-$\beta$-tubulin, Phosphosolutions). (C) Quantification of protein and PAR levels in the immunoblots in panels A and B by densitometry using a Chemidoc imaging system with Quantity One (Bio-Rad). Error bars represent the SEM. U, untreated cells; Q, cells pretreated with the broad-spectrum caspase inhibitor, Q-VD-OPh, at 40 $\mu$M. All the immunoblots shown here were repeated at least twice with similar results.

These results demonstrate a decreased level of and/or delayed activation of caspase-3 in PARG-null TS cells without BZ.

**Increased Levels of PAR in PARG-Null TS Cells without BZ following UV Irradiation.** PAR is synthesized by the PARPs in response to DNA damage. However, the presence of PAR is transient because of the hydrolysis of PAR by PARG. In wild-type TS cells with BZ after treatment with 25 J/m$^2$ of UV radiation, minimal levels of PAR were observed (Figure 2A,d, bracketed region),[a] as expected, because BZ is an inhibitor of PAR synthesis. After 24 h, no significant levels of PAR were observed in these cells as analyzed by immunoblotting (Figure 2A,d) or densitometry (Figure 2C,c). In wild-type TS cells without BZ, PAR synthesis was stimulated by UV, as peak levels were observed after 12 h as quantified by densitometry. However, these levels subsequently decreased, most likely because of the presence of functional PARG in these cells. Interestingly, the presence of activated caspase-3 in wild-type TS cells with or without BZ (Figure 2A,c) appeared to correlate with the time points (12 and 24 h) at which PAR levels were decreased (Figure 2A,d). In PARG-null TS cells with BZ, low levels of PAR were detected at all time points after UV treatment (Figure 2B,d and Figure 2C,c). The levels, however, did not appear to change in response to UV treatment, which is most likely due to the inhibition of PAR synthesis by BZ. In contrast, a time-dependent increase in PAR levels was observed following UV treatment in PARG-null TS cells without BZ, with maximal levels detected at 24 h (Figure 2B,d and Figure 2C,c). In PARG-null TS cells without BZ pretreated with the caspase inhibitor, Q-VD-OPh, PAR levels remained elevated after 24 h (Figure 2B, d, lane Q). Taken together, the results demonstrate the accumulation of PAR in PARG-null TS cells without BZ from 0 to 24 h after UV treatment.

**Decreased Caspase-3/7 Activity and UV Dose-Dependent Increase in PAR Levels in PARG-Null TS Cells without BZ.** Because of the delayed and decreased levels of activated caspase-3 in PARG-null TS cells without BZ following UV treatment, we

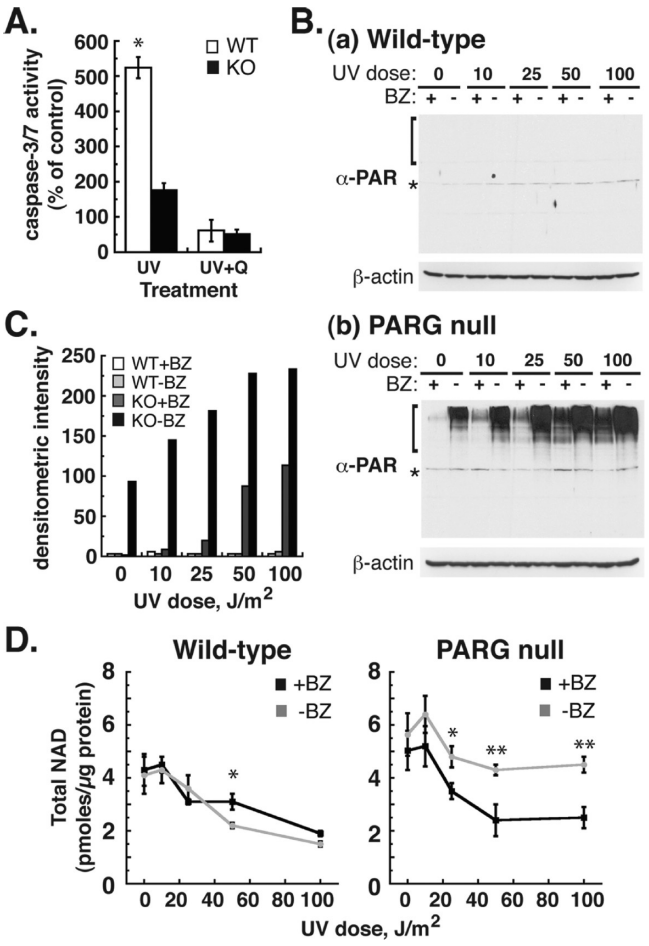


**Figure 3.** Analysis of caspase-3/7 activity, PAR levels, and $NAD^+$ levels in wild-type and PARG-null TS cells after UV treatment. (A) Wild-type and PARG-null TS cells with or without BZ were treated with 25 J/m$^2$ of UV radiation, and 12 h after treatment, $1 \times 10^5$ cells were lysed and analyzed for caspase-3/7 activity using the Apo-ONE Homogeneous Caspase-3/7 Assay (Promega): (□) wild-type TS cells without BZ and (■) PARG-null TS cells without BZ. Q indicates TS cells pretreated with the caspase inhibitor, Q-VD-OPh. Error bars represent the SEM. *$P < 0.01$ between WT-BZ and KO-BZ (one-way ANOVA and unpaired Student's $t$ test). (B) Wild-type (a) and PARG-null TS cells (b) were treated with 10−100 J/m$^2$ of UV radiation, and after 2 h, cell lysates were subjected to the immunoblotting detection of PAR (clone 96-10, Trevigen). Equal loading of each lane was confirmed by the detection of $\beta$-actin. (C) Quantification of PAR levels in the immunoblots in panel B by densitometry using the Chemidoc imaging system with Quantity One (Bio-Rad). (D) Twenty to twenty-four hours after being treated, cells were harvested, and total $NAD^+$ levels were quantified using the alcohol dehydrogenase cycling assay.[34] Total $NAD^+$ levels were expressed in relation to total protein content: (black squares) wild-type or PARG-null TS cells with BZ and (gray squares) wild-type or PARG-null TS cells without BZ. Each sample was assayed in triplicate, and error bars represent SEM. All experiments were performed at least twice with similar results. *$P < 0.05$ between WT with BZ and WT without BZ or PARG-null with BZ and PARG-null without BZ. **$P < 0.01$ between PARG-null with BZ and PARG-null without BZ.

measured total caspase-3/7 activity using a fluorometric caspase-3/7 activity assay. Wild-type and PARG-null TS cells were cultured without BZ for 2 days, treated with 25 J/m$^2$ of UV radiation, and assayed for caspase-3/7 activity after 12 h. The results demonstrate an approximately 5-fold increase in caspase-3/7 activity in wild-type TS cells without BZ following UV radiation (Figure 3A). However, in PARG-null TS cells, caspase-3/7 activity increased only 1.8-fold over that of untreated levels. These results are consistent with the aforementioned activated caspase-3 immunoblot/densitometry results, where activated caspase-3 was detected in wild-type but not PARG-null TS cells without BZ, 12 h after UV irradiation (Figure 2). In the presence of the caspase inhibitor, Q-VD-OPh, caspase-3/7 activity remained below control levels in both wild-type and PARG-null TS cells following UV treatment (Figure 3A). These results provide further evidence that increased levels of PAR due to the absence of PARG lead to a decrease in caspase-3/7 activity after UV irradiation.

To further investigate PAR levels, we next analyzed the levels of PAR following the treatment of wild-type and PARG-null TS cells with 10−100 J/m$^2$ of UV radiation. These cells were cultured with or without BZ for 2 days, and PAR levels were analyzed by Western blotting 2 h later to analyze initial PAR levels (Figure 3B). The results demonstrate the absence of PAR in wild-type TS cells with or without BZ (Figure 3B,a). Analysis of PAR levels in wild-type TS cells from 0 to 2 h after UV irradiation confirmed the absence of PAR in these cells in response to UV radiation (data not shown). In PARG-null TS cells with BZ, significant levels of PAR were detected at each UV dose (Figure 3B,b). Quantification of these PAR levels by densitometry indicated an increase in PAR levels at each dose (Figure 3C). However, in PARG-null TS cells without BZ, a UV dose-dependent increase in PAR levels was also observed by immunoblotting (Figure 3B,b) and densitometry (Figure 3C). However, these PAR levels were significantly higher than in wild-type TS cells with or without BZ and PARG-null TS cells with BZ (Figure 3B,a and Figure 3B,b). At the highest UV dose (100 J/m$^2$), PAR levels in PARG-null TS cells without BZ were approximately 50-fold higher than in wild-type TS cells with or without BZ and more than 2-fold higher than in PARG-null TS cells with BZ (Figure 3C). This demonstrates that UV irradiation induces the synthesis of PAR, which leads to the accumulation of PAR in the absence of PARG.

**Increased Levels of $NAD^+$ in PARG-Null TS Cells without BZ following UV Irradiation.** An additional parameter that was analyzed in these cells was the level of $NAD^+$. $NAD^+$ is the substrate utilized by the PARPs to synthesize PAR.[38] It is also an essential coenzyme in mitochondrial redox reactions and a measure of energy status and the response to DNA damage.[39] For example, it has been postulated that high levels of PAR synthesis can deplete cellular $NAD^+$ levels, which would result in cell death by necrosis.[10] Wild-type and PARG-null TS cells were treated with 10−100 J/m$^2$ of UV radiation as described above, and total $NAD^+$ levels, normalized to total cellular protein, were quantified using the alcohol dehydrogenase (ADH) $NAD^+$ cycling assay.[34] The results demonstrate no significant change in $NAD^+$ content in wild-type TS cells with or without BZ and PARG-null TS cells with BZ after 10 J/m$^2$ (Figure 3D). However, a UV dose-dependent decrease in total $NAD^+$ content is subsequently displayed after the 25−100 J/m$^2$ UV doses. In PARG-null TS cells without BZ, $NAD^+$ levels also do not appear to significantly change after treatment with 10 J/m$^2$ of UV radiation. Surprisingly, the $NAD^+$ levels appear to remain elevated after the 25−100 J/m$^2$ UV doses (Figure 3D). Further, these levels of $NAD^+$ were significantly higher than the $NAD^+$ levels in PARG-null TS cells with BZ and wild-type TS cells with or without BZ. These elevated levels of $NAD^+$ in PARG-null TS

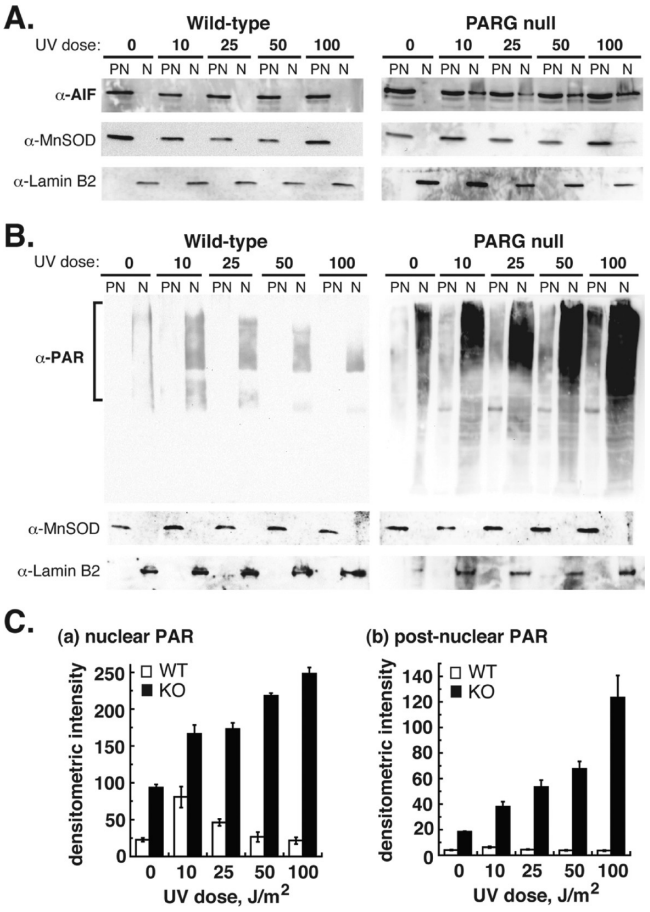


**Figure 4.** Immunoblotting detection of AIF and PAR in wild-type and PARG-null TS cells following UV irradiation. Wild-type and PARG-null TS cells were grown without BZ for 2 days and then treated with 10−100 J/m$^2$ of UV radiation; 16−20 h later, the cells were fractionated into nuclear (N) and postnuclear (PN) compartments by being subjected to 40 strokes in a 2 mL Dounce homogenizer. (A) Immunodetection of AIF (polyclonal anti-AIF, Millipore) in each subcellular fraction. The immunodetection of manganese superoxide dismutase (MnSOD) (monoclonal anti-MnSOD, Millipore) and lamin B2 (monoclonal anti-Lamin B2, Thermo Scientific) was included to indicate successful fractionation of the postnuclear and nuclear compartments, respectively. (B) Immunodetection of PAR (Trevigen) in each subcellular fraction. (C) Quantification of PAR levels in the immunoblots in panel B by densitometry using the Chemidoc imaging system with Quantity One (Bio-Rad). Error bars represent the SEM. Each Western blot was repeated at least twice with similar results.

cells without BZ indicate that the elevated levels of PAR observed in these cells (Figure 3B,b) do not lead to the depletion of $NAD^+$. This suggests that necrosis is not expected to be the primary pathway of cell death in PARG-null TS cells after UV irradiation.

**Mitochondrial-to-Nuclear Translocation of AIF in PARG-Null TS Cells without BZ following UV Irradiation.** Previously published studies demonstrate that cell death induced by PAR is mediated by AIF.[18,21] In PARG-null TS cells, withdrawal of BZ or treatment with small doses of DNA-damaging agents causes PAR accumulation and cell death.[8,9] Thus, to determine if AIF is involved in cell death due to UV radiation in the absence of PARG, wild-type and PARG-null TS cells without BZ were treated as described above with 10−100 J/m$^2$ of UV radiation. AIF is a mitochondrial protein that translocates to the nucleus following apoptotic stimuli.[19] Therefore, the presence of AIF in the nuclear compartment indicates the presence of cell death via AIF.[19,26] After 16−20 h, cells were fractionated into nuclear and postnuclear (cytoplasmic and mitochondrial) fractions by Dounce homogenization, and AIF was analyzed by Western blotting (Figure 4). Successful subcellular fractionations were monitored by the immunoblotting detection of mitochondrial manganese superoxide dismutase (MnSOD) and nuclear lamin B2. In wild-type cells without BZ, no AIF was observed in the nuclear fractions after each UV dose (Figure 4A), which indicates the absence of AIF-mediated cell death. In contrast, in PARG-null TS cells without BZ, AIF was detected in the nuclear fraction at each UV dose, which indicates the presence of AIF-mediated cell death (Figure 4A). The results thus demonstrate the induction of AIF-mediated cell death in PARG-null TS cells without BZ following UV treatment. Because cell death via AIF was not observed in wild-type TS cells without BZ, the activation of this cell death pathway is due to the absence of PARG.

To determine concurrent PAR levels in these cells, we analyzed each subcellular fraction by the immunoblotting detection of PAR (Figure 4B). The results demonstrate the presence of PAR in the nucleus of wild-type TS cells without BZ 16 h after UV irradiation (Figure 4B). No PAR was detected in the postnuclear fractions of these cells. Interestingly, the levels of intranuclear PAR in these cells appeared to decrease with increasing doses of UV, as determined by densitometry (Figure 4C,a). In PARG-null TS cells without BZ, PAR was also present in the nuclear fractions (Figure 4B). Further, these levels of intranuclear PAR were significantly higher at each UV dose as compared to those in wild-type TS cells (Figure 3C,a). Moreover in PARG-null TS cells without BZ, significant levels of PAR were detected in the postnuclear fractions after the UV dose. These postnuclear PAR levels increased with each UV treatment and were maximal after 100 J/m$^2$ (Figure 3C,b), which indicates a UV dose-dependent increase in the level of postnuclear PAR. Because PAR is only synthesized in the nucleus in response to DNA damage, these results thus demonstrate that the high levels of intranuclear PAR in the absence of PARG lead to the presence of PAR in the cytoplasm and/or mitochondria.

Taken together, the results demonstrate the ability of the absence of PARG to induce cell death mediated by AIF following UV-induced DNA damage. Because this pathway is dependent on PAR, the increased levels of PAR due to the absence of PARG in these cells appear to activate this alternative pathway of cell death.

## DISCUSSION

In this study, we demonstrate that the complete absence of PARG leads to the activation of cell death mediated by AIF following UV irradiation. The events associated with this occurrence have a possible effect on caspase-3 functionality, decreased amounts of cleaved PARP-1 and increases in intranuclear and cytoplasmic PAR levels. In addition, although PAR levels are increased because of the absence of PARG, we demonstrate elevated, rather than depleted, levels of $NAD^+$. Taken together, the results demonstrate that the treatment of PARG-null TS cells following UV irradiation leads to the induction of the AIF cell death pathway. Because this AIF pathway was not activated in wild-type TS cells or PARG-null TS cells with BZ, the results suggest that this occurrence is due to elevated levels of PAR. The

findings thus suggest that inhibiting PARG is expected to lead to the induction of cell death mediated by AIF. However, expanding these studies to different cell types and different DNA-damaging treatments will be required to determine the extent of this ability to induce a potentially unique form of cell death.

Since the discovery of AIF in 1996, its established roles in normal cellular function[40,41] and cell death[19,42] have revealed its potential as a therapeutic target.[21,43] However, AIF-mediated cell death is still an emerging topic, as more studies are required to improve our understanding of this pathway. Our contribution here is an improved understanding of the molecular events that occur during the initiation of cell death mediated by AIF. We demonstrate that these events include the alteration of caspase-3 activity, increases in PAR levels, and minimal changes in $NAD^+$ status. In conjunction with these events, we reveal that the primary pathway of cell death in PARG-null TS cells without BZ following UV irradiation appears to be mediated by AIF, while cell death in wild-type TS cells appears to be primarily mediated by other mechanisms. However, caspase-3 activation and cleaved PARP-1 were observed in PARG-null TS cells 24 h after treatment, which suggests a subsequent involvement of caspase-mediated apoptosis in these cells.

The reported ability of the absence of PARG to decrease both caspase-3 activation and caspase-cleaved PARP-1 levels provides further evidence of a role for PAR in the modulation of caspase-3 activity. The possibility exists that increased PARP-1 automodification may cause PARP-1 to be less efficiently cleaved by caspase-3. However, an effect on other caspases is possible. Our studies show decreased caspase-3/7 activity in PARG-null TS cells. In addition, caspase-7 has been shown to preferentially cleave automodified PARP-1.[44,45] Thus, the decreased levels of cleaved PARP-1 may reflect an effect of PAR on caspase-3 and caspase-7 activity. However, future studies will need to be conducted to identify which caspases are affected by PAR.

There are conflicting studies about the effect of PARG inhibition or its absence on cell death. PARG knockdown by RNA interference (RNAi) leads to decreased levels of cell death following $H_2O_2$ treatment.[46] Similar RNAi knockdown of PARG and treatment with $\gamma$ radiation lead to increased levels of cell death.[5] DNA-damaging treatments after disruption of the *Parg* gene lead to increased levels of cell death.[6−8,28] It is possible that these different results with respect to cell death are due to the different PARG isoforms present in the cell. The *Parg* gene is unique, but alternative splicing of PARG mRNA leads to multiple PARG isoforms that localize to different cellular compartments.[47,48] The cellular functions of the extranuclear isoforms are not known, so different cell death phenotypes may result from the selective knockdown of the cytoplasmic or mitochondrial PARGs. Here, we utilize cells that are completely absent of all PARG isoforms, which leads to increased levels of cell death and the activation of the AIF cell death pathway. These studies can be expanded in the future to investigate the effect of each individual PARG isoform on cell death and AIF functionality.

The absence of PAR in wild-type TS cells from 0 to 2 h after UV irradiation is surprising. The low levels of PAR in these cells from 6 to 24 h after UV may reflect PAR synthesis following the caspase-dependent fragmentation of DNA, which could serve to activate PARP. Thus, the formation of PAR in wild-type TS cells could have occurred as a result of secondary effects of UV irradiation.

The different levels of $NAD^+$ in wild-type versus PARG-null TS cells following UV treatment are intriguing. $NAD^+$ is the substrate required for PAR synthesis, and it is a coenzyme that continuously cycles between oxidized ($NAD^+$) and reduced (NADH) forms. The latter role is required in mitochondrial redox reactions, which ultimately lead to the biosynthesis of ATP. In addition, the biosynthesis of $NAD^+$ itself requires ATP.[11] Thus, it is significant that the elevated levels of PAR in PARG-null TS cells without BZ following UV treatment do not lead to decreased levels of $NAD^+$. This suggests no significant effect on the ability to synthesize ATP and the absence of significant levels of necrotic cell death due to the lack of energy depletion. A likely explanation is that the absence of PARG leads to the inhibition of the PARPs via an increased level of automodification. Because PARG is absent, the PARPs remain PAR-modified, which inhibits their ability to utilize $NAD^+$ as a substrate to synthesize more PAR. Further, it suggests an overall different response to UV radiation in PARG-null TS cells versus wild-type TS cells. Because PARG-null TS cells undergo increased amounts of cell death following DNA damage, the $NAD^+$ results alone suggest that the absence of PARG leads to a different pathway of cell death. However, more studies are required to determine if these events are essential for the induction of the AIF cell death pathway. However, from our results, it seems evident that the absence of PARG, which leads to high levels of PAR, does not appear to cause $NAD^+$ depletion.

In summary, we demonstrate the activation of AIF-mediated cell death due to the absence of PARG following UV irradiation. This effect most likely contributes to the phenotype of PARG-null TS cell hypersensitivity to DNA-damaging agents previously reported. Future studies will be required to determine the extent of this AIF activation in other cell types and other DNA-damaging treatments. In addition, more studies are required to determine the therapeutic significance of inducing this alternative cell death pathway.

## ■ ASSOCIATED CONTENT

**Supporting Information.** Figures showing PAR levels 0−2 h after UV treatment in wild-type and PARG-null TS cells and total PAR hydrolysis activity in wild-type and PARG-null TS cells before and after UV treatment. This material is available free of charge via the Internet at http://pubs.acs.org.

## ■ AUTHOR INFORMATION

### Corresponding Author

*Phone: (509) 335-7663. Fax: (509) 335-5902. E-mail: dwkoh@wsu.edu.

### Notes

[a]In Figure 2A,d and Figure 2B,d, the bracketed region represents the normal region of anti-PAR immunodetection following the separation of proteins by 12% SDS−PAGE. This region was utilized in the quantification of PAR levels by densitometry.

[b]In Figure 3B, the bracketed region represents the normal region of anti-PAR immunodetection following the separation of proteins by 7.5% SDS−PAGE. This region was utilized in the quantification of PAR levels by densitometry. The protein band at an $M_r$ of approximately 66000 (denoted by an asterisk) shows the immunodetection of bovine serum albumin (BSA). The production of the anti-PAR (96−10) antibody was accomplished

using methylated BSA as the carrier protein and PAR as the hapten.

### Funding Sources

This work was supported by the American Cancer Society (IRG-77-003-26) and the Pharmaceutical Research and Manufacturers (PhRMA) Foundation.

## ■ ACKNOWLEDGMENT

We give thanks to the laboratory of Dr. Beth A. Vorderstrasse at Washington State University for the use of their UV transilluminator and the laboratory of Dr. Michael J. Smerdon at Washington State University for their general assistance in the UV studies. We also thank Dr. Gary G. Meadows at Washington State University for his critical reading of the manuscript.

## ■ ABBREVIATIONS

PAR, poly(ADP-ribose); PARG, poly(ADP-ribose) glycohydrolase; PARP-1, poly(ADP-ribose) polymerase-1; TS cells, embryonic trophoblast stem cells; BZ, benzamide; $NAD^+$, nicotinamide adenine dinucleotide; CPD, cyclobutane pyrimidine dimer; AIF, apoptosis-inducing factor.

## ■ REFERENCES

(1) Shieh, W. M., Ame, J. C., Wilson, M. V., Wang, Z. Q., Koh, D. W., Jacobson, M. K., and Jacobson, E. L. (1998) Poly(ADP-ribose) polymerase null mouse cells synthesize ADP-ribose polymers. *J. Biol. Chem. 273*, 30069–30072.

(2) Jacobson, M. K., Twehous, D., and Hurley, L. H. (1986) Depletion of nicotinamide adenine dinucleotide in normal and xeroderma pigmentosum fibroblast cells by the antitumor drug CC-1065. *Biochemistry 25*, 5929–5932.

(3) Koh, D. W., Patel, C. N., Ramsinghani, S., Slama, J. T., Oliveira, M. A., and Jacobson, M. K. (2003) Identification of an inhibitor binding site of poly(ADP-ribose) glycohydrolase. *Biochemistry 42*, 4855–4863.

(4) Juarez-Salinas, H., Sims, J. L., and Jacobson, M. K. (1979) Poly(ADP-ribose) levels in carcinogen-treated cells. *Nature 282*, 740–741.

(5) Ame, J. C., Fouquerel, E., Gauthier, L. R., Biard, D., Boussin, F. D., Dantzer, F., de Murcia, G., and Schreiber, V. (2009) Radiation-induced mitotic catastrophe in PARG-deficient cells. *J. Cell Sci. 122*, 1990–2002.

(6) Cortes, U., Tong, W. M., Coyle, D. L., Meyer-Ficca, M. L., Meyer, R. G., Petrilli, V., Herceg, Z., Jacobson, E. L., Jacobson, M. K., and Wang, Z. Q. (2004) Depletion of the 110-kilodalton isoform of poly(ADP-ribose) glycohydrolase increases sensitivity to genotoxic and endotoxic stress in mice. *Mol. Cell. Biol. 24*, 7163–7178.

(7) Fujihara, H., Ogino, H., Maeda, D., Shirai, H., Nozaki, T., Kamada, N., Jishage, K., Tanuma, S., Takato, T., Ochiya, T., Sugimura, T., and Masutani, M. (2009) Poly(ADP-ribose) glycohydrolase deficiency sensitizes mouse ES cells to DNA damaging agents. *Curr. Cancer Drug Targets 9*, 953–962.

(8) Koh, D. W., Lawler, A. M., Poitras, M. F., Sasaki, M., Wattler, S., Nehls, M. C., Stoger, T., Poirier, G. G., Dawson, V. L., and Dawson, T. M. (2004) Failure to degrade poly(ADP-ribose) causes increased sensitivity to cytotoxicity and early embryonic lethality. *Proc. Natl. Acad. Sci. U.S.A. 101*, 17699–17704.

(9) Zhou, Y., Feng, X., and Koh, D. W. (2010) Enhanced DNA accessibility and increased DNA damage induced by the absence of poly(ADP-ribose) hydrolysis. *Biochemistry 49*, 7360–7366.

(10) Berger, N. A. (1985) Poly(ADP-ribose) in the cellular response to DNA damage. *Radiat. Res. 101*, 4–15.

(11) Zhang, J., Dawson, V. L., Dawson, T. M., and Snyder, S. H. (1994) Nitric oxide activation of poly(ADP-ribose) synthetase in neurotoxicity. *Science 263*, 687–689.

(12) Alano, C. C., Garnier, P., Ying, W., Higashi, Y., Kauppinen, T. M., and Swanson, R. A. (2010) $NAD^+$ depletion is necessary and sufficient for poly(ADP-ribose) polymerase-1-mediated neuronal death. *J. Neurosci. 30*, 2967–2978.

(13) Zong, W. X., Ditsworth, D., Bauer, D. E., Wang, Z. Q., and Thompson, C. B. (2004) Alkylating DNA damage stimulates a regulated form of necrotic cell death. *Genes Dev. 18*, 1272–1282.

(14) Lazebnik, Y. A., Kaufmann, S. H., Desnoyers, S., Poirier, G. G., and Earnshaw, W. C. (1994) Cleavage of poly(ADP-ribose) polymerase by a proteinase with properties like ICE. *Nature 371*, 346–347.

(15) Wang, Z. Q., Stingl, L., Morrison, C., Jantsch, M., Los, M., Schulze-Osthoff, K., and Wagner, E. F. (1997) PARP is important for genomic stability but dispensable in apoptosis. *Genes Dev. 11*, 2347–2358.

(16) Simbulan-Rosenthal, C. M., Rosenthal, D. S., Iyer, S., Boulares, A. H., and Smulson, M. E. (1998) Transient poly(ADP-ribosyl)ation of nuclear proteins and role of poly(ADP-ribose) polymerase in the early stages of apoptosis. *J. Biol. Chem. 273*, 13703–13712.

(17) Smulson, M. E., Pang, D., Jung, M., Dimtchev, A., Chasovskikh, S., Spoonde, A., Simbulan-Rosenthal, C., Rosenthal, D., Yakovlev, A., and Dritschilo, A. (1998) Irreversible binding of poly(ADP)ribose polymerase cleavage product to DNA ends revealed by atomic force microscopy: Possible role in apoptosis. *Cancer Res. 58*, 3495–3498.

(18) Yu, S. W., Wang, H., Poitras, M. F., Coombs, C., Bowers, W. J., Federoff, H. J., Poirier, G. G., Dawson, T. M., and Dawson, V. L. (2002) Mediation of poly(ADP-ribose) polymerase-1-dependent cell death by apoptosis-inducing factor. *Science 297*, 259–263.

(19) Susin, S. A., Lorenzo, H. K., Zamzami, N., Marzo, I., Snow, B. E., Brothers, G. M., Mangion, J., Jacotot, E., Costantini, P., Loeffler, M., Larochette, N., Goodlett, D. R., Aebersold, R., Siderovski, D. P., Penninger, J. M., and Kroemer, G. (1999) Molecular characterization of mitochondrial apoptosis-inducing factor. *Nature 397*, 441–446.

(20) Artus, C., Boujrad, H., Bouharrour, A., Brunelle, M. N., Hoos, S., Yuste, V. J., Lenormand, P., Rousselle, J. C., Namane, A., England, P., Lorenzo, H. K., and Susin, S. A. (2010) AIF promotes chromatinolysis and caspase-independent programmed necrosis by interacting with histone H2AX. *EMBO J. 29*, 1585–1599.

(21) Wang, H., Yu, S. W., Koh, D. W., Lew, J., Coombs, C., Bowers, W., Federoff, H. J., Poirier, G. G., Dawson, T. M., and Dawson, V. L. (2004) Apoptosis-inducing factor substitutes for caspase executioners in NMDA-triggered excitotoxic neuronal death. *J. Neurosci. 24*, 10963–10973.

(22) Arnoult, D., Gaume, B., Karbowski, M., Sharpe, J. C., Cecconi, F., and Youle, R. J. (2003) Mitochondrial release of AIF and EndoG requires caspase activation downstream of Bax/Bak-mediated permeabilization. *EMBO J. 22*, 4385–4399.

(23) Arnoult, D., Parone, P., Martinou, J. C., Antonsson, B., Estaquier, J., and Ameisen, J. C. (2002) Mitochondrial release of apoptosis-inducing factor occurs downstream of cytochrome c release in response to several proapoptotic stimuli. *J. Cell Biol. 159*, 923–929.

(24) Cande, C., Vahsen, N., Garrido, C., and Kroemer, G. (2004) Apoptosis-inducing factor (AIF): Caspase-independent after all. *Cell Death Differ. 11*, 591–595.

(25) Xiao, C. Y., Chen, M., Zsengeller, Z., and Szabo, C. (2004) Poly(ADP-ribose) polymerase contributes to the development of myocardial infarction in diabetic rats and regulates the nuclear translocation of apoptosis-inducing factor. *J. Pharmacol. Exp. Ther. 310*, 498–504.

(26) Andrabi, S. A., Kim, N. S., Yu, S. W., Wang, H., Koh, D. W., Sasaki, M., Klaus, J. A., Otsuka, T., Zhang, Z., Koehler, R. C., Hurn, P. D., Poirier, G. G., Dawson, V. L., and Dawson, T. M. (2006) Poly(ADP-ribose) (PAR) polymer is a death signal. *Proc. Natl. Acad. Sci. U.S.A. 103*, 18308–18313.

(27) Ono, T., Kasamatsu, A., Oka, S., and Moss, J. (2006) The 39-kDa poly(ADP-ribose) glycohydrolase ARH3 hydrolyzes O-acetyl-

ADP-ribose, a product of the Sir2 family of acetyl-histone deacetylases. *Proc. Natl. Acad. Sci. U.S.A. 103*, 16687–16691.

(28) Hanai, S., Kanai, M., Ohashi, S., Okamoto, K., Yamada, M., Takahashi, H., and Miwa, M. (2004) Loss of poly(ADP-ribose) glycohydrolase causes progressive neurodegeneration in *Drosophila melanogaster*. *Proc. Natl. Acad. Sci. U.S.A. 101*, 82–86.

(29) Min, W., Cortes, U., Herceg, Z., Tong, W. M., and Wang, Z. Q. (2010) Deletion of the nuclear isoform of poly(ADP)-ribose glycohydrolase (PARG) reveals its function in DNA repair, genomic stability and tumorigenesis. *Carcinogenesis 31*, 2058–2065.

(30) Murad, A. O., de Cock, J., Brown, D., and Smerdon, M. J. (1995) Variations in transcription-repair coupling in mouse cells. *J. Biol. Chem. 270*, 3949–3957.

(31) Smerdon, M. J., and Thoma, F. (1990) Site-specific DNA repair at the nucleosome level in a yeast minichromosome. *Cell 61*, 675–684.

(32) Boulton, S., Pemberton, L. C., Porteous, J. K., Curtin, N. J., Griffin, R. J., Golding, B. T., and Durkacz, B. W. (1995) Potentiation of Temozolomide-induced cytotoxicity: A comparative study of the biological effects of poly(ADP-ribose) polymerase inhibitors. *Br. J. Cancer 72*, 849–856.

(33) Caserta, T. M., Smith, A. N., Gultice, A. D., Reedy, M. A., and Brown, T. L. (2003) Q-VD-OPh, a broad spectrum caspase inhibitor with potent antiapoptotic properties. *Apoptosis 8*, 345–352.

(34) Jacobson, E. L., and Jacobson, M. K. (1997) Tissue NAD as a biochemical measure of niacin status in humans. *Methods Enzymol. 280*, 221–230.

(35) Thiagarajan, P., and Tait, J. F. (1990) Binding of annexin V/placental anticoagulant protein I to platelets. Evidence for phosphatidylserine exposure in the procoagulant response of activated platelets. *J. Biol. Chem. 265*, 17420–17423.

(36) Fadok, V. A., Voelker, D. R., Campbell, P. A., Cohen, J. J., Bratton, D. L., and Henson, P. M. (1992) Exposure of phosphatidylserine on the surface of apoptotic lymphocytes triggers specific recognition and removal by macrophages. *J. Immunol. 148*, 2207–2216.

(37) Faleiro, L., Kobayashi, R., Fearnhead, H., and Lazebnik, Y. (1997) Multiple species of CPP32 and Mch2 are the major active caspases present in apoptotic cells. *EMBO J. 16*, 2271–2281.

(38) Okayama, H., Edson, C. M., Fukushima, M., Ueda, K., and Hayaishi, O. (1977) Purification and properties of poly(adenosine diphosphate ribose) synthetase. *J. Biol. Chem. 252*, 7000–7005.

(39) Jacobson, E. L., Shieh, W. M., and Huang, A. C. (1999) Mapping the role of NAD metabolism in prevention and treatment of carcinogenesis. *Mol. Cell. Biochem. 193*, 69–74.

(40) Pospisilik, J. A., Knauf, C., Joza, N., Benit, P., Orthofer, M., Cani, P. D., Ebersberger, I., Nakashima, T., Sarao, R., Neely, G., Esterbauer, H., Kozlov, A., Kahn, C. R., Kroemer, G., Rustin, P., Burcelin, R., and Penninger, J. M. (2007) Targeted deletion of AIF decreases mitochondrial oxidative phosphorylation and protects from obesity and diabetes. *Cell 131*, 476–491.

(41) Vahsen, N., Cande, C., Briere, J. J., Benit, P., Joza, N., Larochette, N., Mastroberardino, P. G., Pequignot, M. O., Casares, N., Lazar, V., Feraud, O., Debili, N., Wissing, S., Engelhardt, S., Madeo, F., Piacentini, M., Penninger, J. M., Schagger, H., Rustin, P., and Kroemer, G. (2004) AIF deficiency compromises oxidative phosphorylation. *EMBO J. 23*, 4679–4689.

(42) Cregan, S. P., Fortin, A., MacLaurin, J. G., Callaghan, S. M., Cecconi, F., Yu, S. W., Dawson, T. M., Dawson, V. L., Park, D. S., Kroemer, G., and Slack, R. S. (2002) Apoptosis-inducing factor is involved in the regulation of caspase-independent neuronal cell death. *J. Cell Biol. 158*, 507–517.

(43) Cregan, S. P., Dawson, V. L., and Slack, R. S. (2004) Role of AIF in caspase-dependent and caspase-independent cell death. *Oncogene 23*, 2785–2796.

(44) Germain, M., Affar, E. B., D'Amours, D., Dixit, V. M., Salvesen, G. S., and Poirier, G. G. (1999) Cleavage of automodified poly(ADP-ribose) polymerase during apoptosis. Evidence for involvement of caspase-7. *J. Biol. Chem. 274*, 28379–28384.

(45) Pleschke, J. M., Kleczkowska, H. E., Strohm, M., and Althaus, F. R. (2000) Poly(ADP-ribose) binds to specific domains in DNA damage checkpoint proteins. *J. Biol. Chem. 275*, 40974–40980.

(46) Blenn, C., Althaus, F. R., and Malanga, M. (2006) Poly(ADP-ribose) glycohydrolase silencing protects against $H_2O_2$-induced cell death. *Biochem. J. 396*, 419–429.

(47) Meyer, R. G., Meyer-Ficca, M. L., Whatcott, C. J., Jacobson, E. L., and Jacobson, M. K. (2007) Two small enzyme isoforms mediate mammalian mitochondrial poly(ADP-ribose) glycohydrolase (PARG) activity. *Exp. Cell Res. 313*, 2920–2936.

(48) Meyer-Ficca, M. L., Meyer, R. G., Coyle, D. L., Jacobson, E. L., and Jacobson, M. K. (2004) Human poly(ADP-ribose) glycohydrolase is expressed in alternative splice variants yielding isoforms that localize to different cell compartments. *Exp. Cell Res. 297*, 521–532.